THE JOURNAL OF BIOLOGICAL CHEMISTRY VOL. 285, NO. 15, pp. 11402–11410, April 9, 2010

A Novel Protease-activated Receptor-1 Interactor, Bicaudal D1, Regulates G Protein Signaling and Internalization*[S]

Received for publication, January 20, 2010 Published, JBC Papers in Press, February 17, 2010, DOI 10.1074/jbc.M110.105403

Steven Swift, Jian Xu, Vishal Trivedi, Karyn M. Austin, Sarah L. Tressel, Lei Zhang, Lidija Covic, and Athan Kuliopulos[1]

From the Molecular Oncology Research Institute, Tufts Medical Center, and Departments of Biochemistry and Medicine, Tufts University School of Medicine, Boston, Massachusetts 02111

Protease-activated receptor-1 (PAR1) is a G protein-coupled receptor that plays critical roles in cancer, angiogenesis, inflammation, and thrombosis. Proteolytic cleavage of the extracellular domain of PAR1 generates a tethered ligand that activates PAR1 in an unusual intramolecular mode. The signal emanating from the irreversibly cleaved PAR1 is terminated by G protein uncoupling and internalization; however, the mechanisms of PAR1 signal shut off still remain unclear. Using a yeast two-hybrid screen, we identified Bicaudal D1 (BicD1) as a direct interactor with the C-terminal cytoplasmic domain of PAR1. *BICD* was originally identified as an essential developmental gene associated with mRNA and Golgi-endoplasmic reticulum transport. We discovered a novel function of BicD1 in the modulation of G protein signaling, cell proliferation, and endocytosis downstream of PAR1. BicD1 and its C-terminal CC3 domain inhibited PAR1 signaling to G_q-phospholipase C-β through coiled-coil interactions with the cytoplasmic 8th helix of PAR1. Unexpectedly, BicD1 was also found to be a potent suppressor of PAR1-driven proliferation of breast carcinoma cells. The growth-suppressing effects of BicD1 required the ability to interact with the 8th helix of PAR1. Silencing of BicD1 expression impaired endocytosis of PAR1, and BicD1 co-localized with PAR1 and tubulin, implicating BicD1 as an important adapter protein involved in the transport of PAR1 from the plasma membrane to endosomal vesicles. Together, these findings provide a link between PAR1 signal termination and internalization through the non-G protein effector, BicD1.

The protease-activated receptors (PARs)[2] are a family of G protein-coupled receptors that play diverse roles in normal and pathophysiologic processes, including hemostasis, thrombosis, angiogenesis, inflammation, and cancer (1). PAR1 is one of four protease-activated receptors (PAR1–4) that has been shown to respond to specific proteases, including thrombin, activated protein C, plasmin, and matrix metalloprotease-1 (2–6). Proteolytic cleavage exposes a tethered ligand that binds to the body of the receptor to induce transmembrane signaling through intracellular G proteins G_q, G_i, and $G_{12/13}$ (7). The irreversible cleavage of PAR1 and generation of a tethered ligand raise questions as to what proteins or processes are involved in controlling a potentially unregulated G protein signal. Uncontrolled PAR1-G protein signaling in carcinoma cells may contribute to hyperplasia, angiogenesis, and tumor growth (5, 8). In the vasculature, excess PAR1 signaling leads to restenosis, cardiomyocyte hypertrophy, and pathologic cardiac remodeling (9, 10).

Non-G protein effectors have been shown to play critical roles in modulating G protein-coupled receptor function, and they provide texture to the intracellular signal (11). The β-arrestins are important effector molecules involved in termination of receptor signaling and the initiation of mitogen-activated protein kinase signaling cascades (12, 13). Activated PAR1 is desensitized by phosphorylation of its cytoplasmic tail by G protein-coupled receptor kinases GRK-3 and GRK-5 and by the binding of β-arrestin (14–17). Interestingly, although β-arrestin mediates uncoupling of PAR1 from phospholipase C (PLC)-β signaling, internalization of PAR1 occurs through a pathway independent of β-arrestin (17, 18). Following internalization, endosomes harboring activated PAR1 are targeted to the lysosomes through sorting nexin-1, which results in permanent removal of the irreversibly cleaved PAR1 (19, 20). Unlike PAR2, which requires β-arrestin to be endocytosed (13), ligand-activated PAR1 is internalized via a dynamin- and clathrin-dependent pathway; however, the mechanism still remains unclear (21). An unknown adapter protein that binds directly to PAR1 may be involved in recruiting activated PAR1 to clathrin-coated pits to initiate endocytosis.

To identify novel proteins involved in regulating the G protein signaling and internalization of PAR1, we performed a yeast two-hybrid screen using the C-terminal cytoplasmic tail of PAR1 as bait. From a screen of an embryonic cDNA library, we identified the C-terminal coiled-coil 3 domain of Bicaudal D1 (BicD1) as a potential interactor with PAR1. *BicD1* is the human homolog of the *Drosophila* Bicaudal D gene (*BICD*). *BICD* was originally identified as a developmental gene associated with mRNA and Golgi-endoplasmic reticulum transport in *Drosophila* and mammalian cells (22–26). We found that endogenous BicD1 strongly interacts with the C-terminal cytoplasmic domain of PAR1, which inhibits signaling to G_q-PLC-β pathways. Knockdown of

* This work was supported, in whole or in part, by National Institutes of Health Grants F32 HL10296 (to S. S.), T32 CA65441 (to L. Z.), and R01-HL64701, R01-CA122992, and R01-HL57905 (to A. K.). This work was also supported by the Susan G. Komen Breast Cancer Foundation (A. K.).

[S] The on-line version of this article (available at http://www.jbc.org) contains supplemental Fig. 1.

[1] To whom correspondence should be addressed: Tufts Medical Center, Box 7510, 750 Washington St., Boston, MA 02111. Tel.: 617-636-8482; Fax: 617-636-7855; E-mail: athan.kuliopulos@tufts.edu.

[2] The abbreviations used are: PAR, protease-activated receptor; PLC, phospholipase C; BicD1, Bicaudal D1; EGFP, enhanced green fluorescent protein; InsP, inositol phosphate; FACS, fluorescence-activated cell sorter; WT, wild type; as, antisense.

BicD1 expression blocked endocytosis of ligand-activated PAR1. BicD1 was also found to be a potent suppressor of PAR1-dependent proliferation of breast carcinoma cells. Together, these findings reveal BicD1 to be a non-G protein effector of PAR1 that controls G protein signaling, endocytosis, and proliferation.

EXPERIMENTAL PROCEDURES

Cell Culture and Reagents—COS7, MCF-7, HeLa, and Rat1 fibroblasts were maintained in Dulbecco's modified Eagle's medium supplemented with 10% fetal bovine serum and 1% penicillin and streptomycin (Invitrogen) in 5% CO_2 at 37 °C. Human α-thrombin was purchased from Hematologic Technologies. Peptides SFLLRN, TFLLRN, and AYPGKF were synthesized with C-terminal amides by the Tufts Peptide Core Facility.

Yeast Two-hybrid Screening—DNA encoding the last 53 amino acids of human PAR1 was cloned into the "bait" vector pPC97. The resulting vector pPC97-P1CT was transformed in yeast strain MVa203. MVa203 carrying pPC97-P1CT, expressing GAL4-DNA-binding domain-PAR1 cytoplasmic tail, was transformed with a mouse embryo cDNA library fused to the GAL4 activation domain. Similarly, DNA encoding the last 42 amino acid residues of human PAR4 was cloned into pPC97. Transformants with interacting clones were selected by growth on histidine-free and uracil-free synthetic media supplemented with 50 mM 3-aminotriazole. Colonies were then tested for lacZ activity by a blue/white screen with 5-bromo-4-chloro-3-indolyl-β-D-galactopyranoside. Plasmids were isolated and retested in yeast transformed with empty bait vector, PAR4 cytoplasmic tail, or the PAR1 cytoplasmic tail for growth on selective media.

Mammalian Expression Construct—The mouse *BicD1* (*mBicD1*) gene fragment (C-terminal 231 amino acids) was cloned into pEGFP-C1 (Clontech) to make GFP-BicD1ct for expression in COS7 cells. The human *BicD1* (*hBicD1*) fragment encoding the N-terminal coiled-coil domains 1 and 2 was PCR-amplified from a human aorta cDNA library (Clontech). DNA encoding the N-terminal 653 amino acids of *hBicD1* was fused to DNA encoding the 220 C-terminal amino acids of *mBicD1* to yield a full-length chimeric *BicD1* encoding an 873-amino acid protein. A single potential difference is present at residue 588, where published sequences have a proline; our sequencing data indicate that BicD1 has an alanine at residue 588. According to the DNA sequence in the human genome data base, BicD1 residue 588 is an alanine. Within the 220-amino acid mBicD1 fragment, there are 8 amino acid differences between our mouse sequence and the human sequence in the genome data base (NCBI). The differences are as follows (human/mouse): S826P, V827D, T844I, N846T, T866V, W869C, P870T, D871G. The *BicD1* gene was cloned into the mammalian expression vector pCDEF3 with a T7 epitope tag introduced at the 5′ end of *BicD1* to make pCDEF3-T7-BicD1. Antisense DNA encoding position 904 to 79 of *BicD1* (asBicD1) was subcloned into pcDEF3 vector. An antisense enhanced green fluorescence protein (asEGFP) was used as a second negative control, made by cloning an antisense EGFP sequence from bp 760 to the ATG start site by PCR from the pEGFP plasmid (Clontech), and two restriction sequences (XbaI, BamHI) were added onto each end of the product. The sequence was then inserted into the pcDEF3 vector resulting in a pcDEF3-asEGFP construct.

Immunoprecipitation and Western Blot Analysis—BicD1 cytoplasmic tail peptide [Ac]-EDLEFDHEQSRRSKC-[NH_2] was coupled to keyhole limpet hemocyanin to use as an antigen for production of rabbit polyclonal antibody (Strategic BioSolutions). The rabbit polyclonal PAR1 antibody (SFLLR-Ab) was generated as described previously (3). Rat1 cells were lysed in immunoprecipitation buffer (1% Triton X-100, 50 mM Tris, pH 7.4, 100 mM NaCl, 5 mM EDTA, 50 mM NaF, and 1 mM phenylmethylsulfonyl fluoride). FLAG-PAR1 was immunoprecipitated from Rat1 lysates by anti-FLAG antibody M2-agarose beads (Sigma) and eluted with 0.1 M glycine, pH 3.4. Eluates were neutralized with Tris-HCl, pH 8.0, and resolved by 10% SDS-PAGE. Proteins were transferred electrophoretically to polyvinylidene difluoride membranes (Millipore). Western blots were probed with anti-BicD1 serum (1:1000 dilution) or with anti-PAR1 serum (1:1000 dilution) or with anti-T7 tag monoclonal antibody (1:2000 dilution; Novagen, Madison, WI). Immunoreactive bands were detected by enhanced chemiluminescence (Amersham Biosciences).

Inositol Phosphate (InsP) Production Assay—InsP production assays were carried out as described previously (27). Briefly, COS7 or Rat1 fibroblasts expressing PAR1 were plated into 12-well plates at 250,000 cells/well. ^{3}H-Labeled myoinositol (2 mCi/ml; Amersham Biosciences) was added to the cells, and 24 h later wells were rinsed twice with 2 ml of Dulbecco's modified Eagle's medium containing 10 mM HEPES, pH 7.3, then twice with 2 ml of phosphate-buffered saline containing 20 mM LiCl. Cells were stimulated with agonist (in triplicate) for 30 min and then extracted with cold methanol and chloroform. Extracts were loaded onto columns containing 1 ml of anion exchange resin AG1X8, formate form, 100–200 mesh size (Bio-Rad). The columns were then washed twice with 10 ml of H_2O and twice with 10 ml of 60 mM ammonium formate/5 mM Borax. InsP was eluted with 4 ml of 2 M ammonium formate/0.1 M formic acid. Samples were mixed with 7.5 ml of scintillation fluid and counted.

Confocal Microscopy—COS7 cells transfected with T7-BicD1 and/or PAR1 were lifted the next day using 2 mM EDTA-phosphate-buffered saline and replated onto sterile coverslips. The cells were then grown an additional 40–48 h before fixing with 2% formaldehyde. PAR1 was detected by 1:100 antiPAR1 rabbit IgG with 1:100 fluorescein isothiocyanate goat anti-rabbit IgG (Zymed Laboratories, Inc.). T7-BicD1 was detected by 1:100 anti-T7 mouse monoclonal antibody with 1:100 rhodamine goat anti-mouse IgG (Molecular Probes). Confocal images were then collected.

PAR1 Endocytosis Assay—COS7 cells were transfected with T7-PAR1 cDNA ± BicD1 cDNA. HeLa cells were transfected with T7-PAR1 cDNA ± antisense BicD1 (asBicD1) or pcDEF3 vector. Two days after transfection, cells were lifted with 2 mM EDTA-phosphate-buffered saline. For endocytosis assay, 5×10^5 cells in phosphate-buffered saline were used/assay tube. Cells were probed with 1:200 anti-T7 mouse monoclonal antibody followed by treatment with 100 μM TFLLRN. At the indi-

A

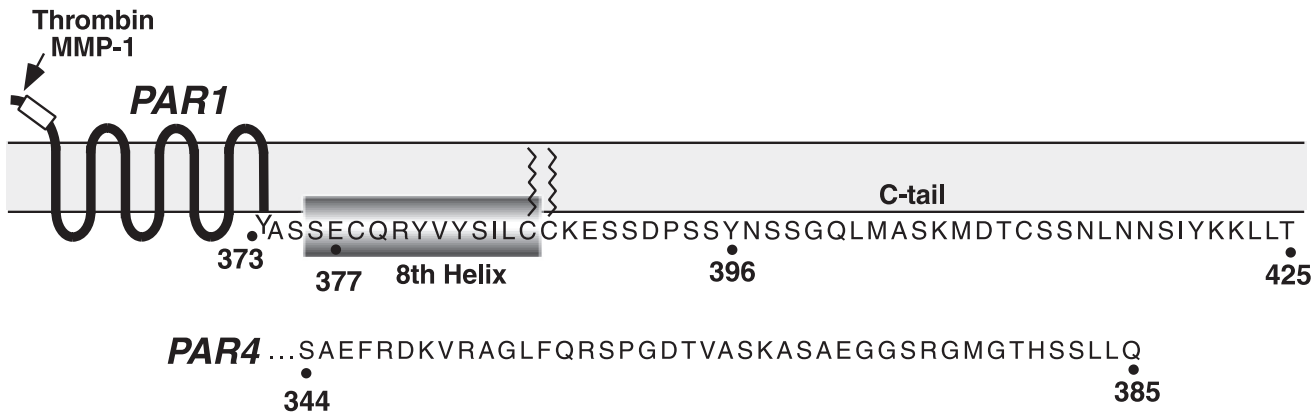

B

Mouse Embryo cDNA Library

Bait	PAR1 373-425	PAR4 344-385
Transformants	3×10^6	1×10^7
His+ Ura+ colonies	184	80
LacZ+ colonies	19	0
LacZ+ on retest	9	0

C

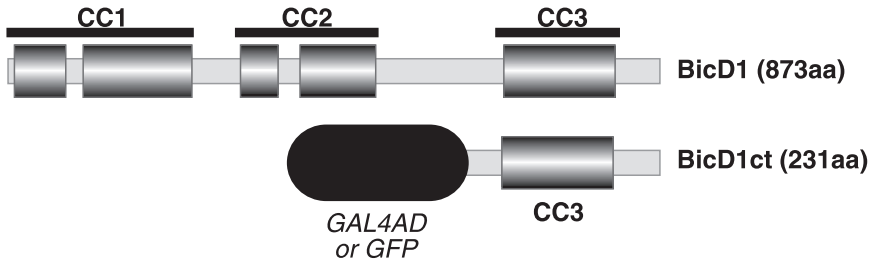

D

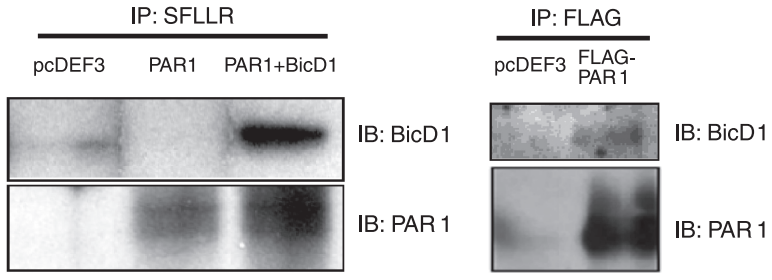

FIGURE 1. **BicD1 associates with the C-terminal cytoplasmic domain of PAR1.** *A*, model depicting the C-terminal cytoplasmic domains of PAR1 and PAR4 is shown. *B*, yeast two-hybrid screen of a mouse embryo cDNA library was conducted using GAL4DB-PAR1(373–425) or GAL4DB-PAR4(344–385) as the bait proteins. *C*, C-terminal CC3 domain of mBicD1, BicD1ct, was found to interact with GAL4DB-PAR1(373–425). Full-length BicD1 has three coiled-coil domains, CC1, CC2, and CC3. *D*, *left immunoloblots*, PAR1 was immunoprecipitated (*IP*) with the SFLLR antibody from COS7 cell lysates co-transfected with PAR1 and T7-BicD1, or pcDEF3 vector control. *Right immunoblots*, endogenous BicD1 was co-immunoprecipitated with the M2 FLAG antibody from Rat1 fibroblasts lysates stably transfected with FLAG-PAR1 and the blots stained with the BicD1 antibody or the SFLLR antibody, as indicated.

cated time points, formaldehyde was added to the cells to a final concentration of 1.3%, and the cells were immediately placed on ice. Cells were then labeled with 1:100 fluorescein isothiocyanate goat anti-mouse IgG (Zymed Laboratories, Inc.), and PAR1 surface levels were determined by using a FACScan flow cytometer (Becton Dickinson). Cells probed with secondary antibody alone were used to determine background fluorescence.

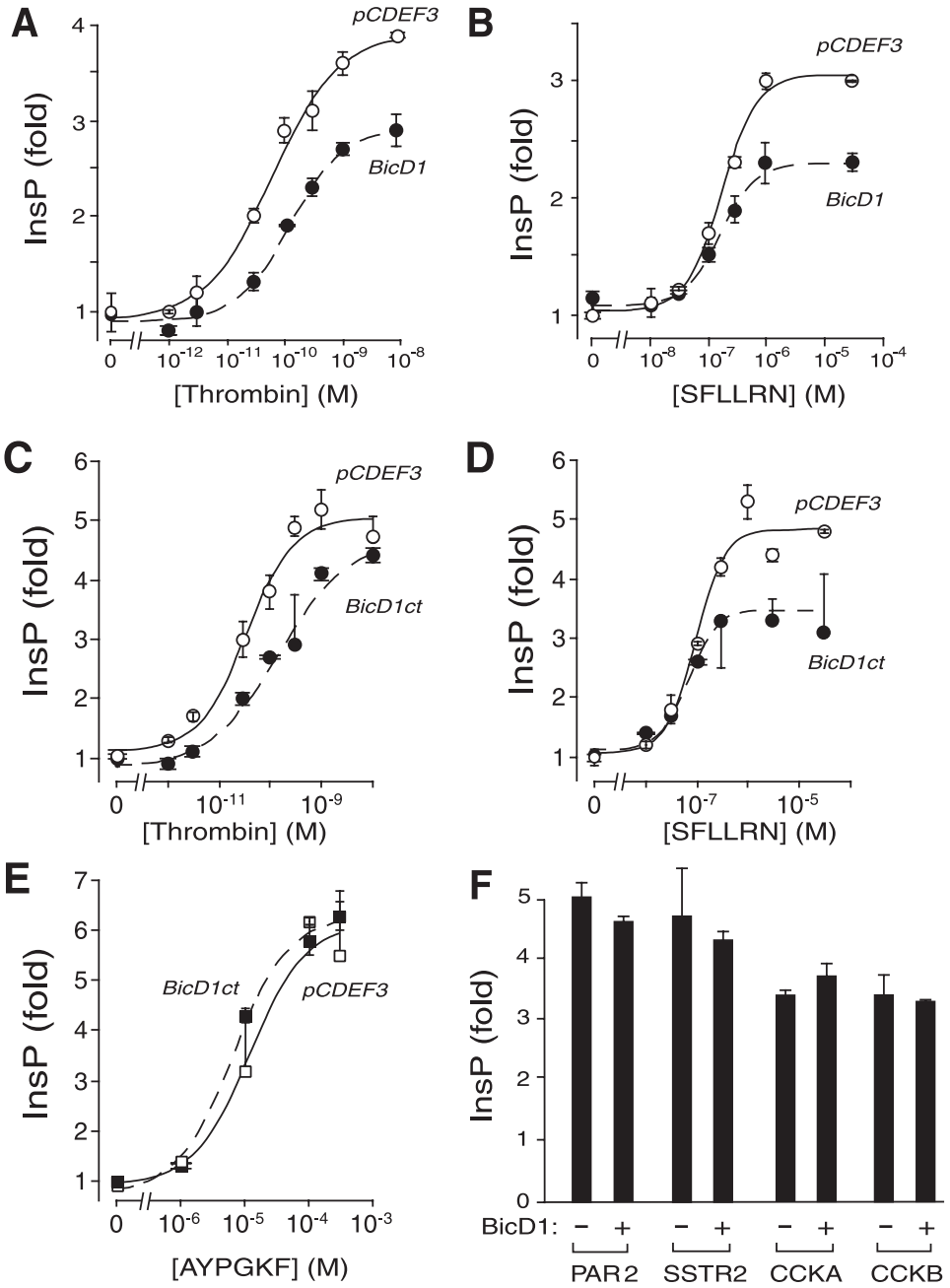

FIGURE 2. **BicD1 specifically inhibits PAR1-G protein signaling.** *A–D*, WT PAR1 was co-transfected into COS7 cells along with full-length BicD1(1–873), GFP-BicD1ct (BicD1ct), or pCDEF3 vector control as indicated. Cells were then challenged for 30 min with 1 pM to 10 nM thrombin, or 10 nM to 30 μM SFLLRN agonists (each *point* done in triplicate). PLC-β activity was determined by measuring total [^{3}H]InsP formation and converted to fold response relative to buffer alone. Experiments were conducted at least three times. *E*, WT PAR4 was co-transfected into COS7 cells along with GFP-BicD1ct or pCDEF3 vector control and PLC-β activity was determined as above except that AYPGKF was used as agonist. *F*, full-length BicD1 (+) or pCDEF3 vector (−) was co-transfected into COS7 cells along with PAR2, SSTR2, CCKA, or CCKB receptors, and PLC-β activity was determined as above. The agonists used were 10 μM SLIGKV for PAR2, 1 μM AGCKNFFWKTFTSC for SSTR2, 300 nM CCK-8 for CCKA and CCKB. Data are plotted as mean ± 1 S.D. (*error bars*).

RESULTS

Interactions between PAR1 and BicD1—The C-terminal cytoplasmic domains of the PAR1 and PAR4 receptors were used as bait in a yeast two-hybrid screen to find potential interacting proteins from a mouse embryonic cDNA library (Fig. 1, *A* and *B*). After secondary screening, there were no candidate interactors for the PAR4 C-terminal tail; however, nine clones remained positive for the PAR1 C-terminal cytoplasmic domain bait. Two of these putative PAR1-interacting clones encoded the C-terminal CC3 domain of BicD1. The other seven clones encoded small peptides and were not pursued further.

A human *BicD1* fragment encoding the N-terminal coiled-coil domains 1 and 2 (residues 1–653, with N-terminal T7 epitope tag) was cloned from a human aorta cDNA library and fused to DNA encoding the 220 residue CC3 domain of *mBicD1* to yield full-length *BicD1* (Fig. 1*C*). To validate the interaction between PAR1 and BicD1, we tested whether PAR1 and BicD1 would form a stable complex when co-expressed in COS7 fibroblasts. As shown in Fig. 1*D*, BicD1 co-immunoprecipitated with PAR1 in cells co-expressing both constructs but failed to pull down BicD1 in pcDEF3 vector control. Conversely, we were able to immunoprecipitate BicD1 with FLAG-tagged PAR1 from Rat1 fibroblasts that were stably expressing PAR1 but not from Rat1 cells that lacked PAR1. This indicates that BicD1 stably interacts with full-length PAR1 in mammalian cells.

Full-length BicD1 and the BicD1 CC3 Domain Specifically Inhibit Signaling between PAR1 and G Protein—The C-terminal i4 domain of PAR1 is required for signaling to G proteins (27), therefore we tested whether BicD1 would affect PAR1-G protein coupling. PAR1 and full-length BicD1 or the BicD1 CC3 domains (BicD1ct) were co-expressed in COS7 fibroblasts. The effect of BicD1 on coupling of PAR1 to G_q was assessed using a well characterized PLC-β-dependent InsP assay (27). PAR1 stimulates PLC-β signaling by directly activating G_q α-subunits in COS7 fibroblasts. As shown in Fig. 2, *A* and *B*, transfection of COS7 fibrobasts with BicD1 caused a 30–40% inhibition of the maximal InsP signaling upon stimulation with thrombin or the synthetic peptide ligand SFLLRN. Likewise, co-expression of PAR1 with the BicD1ct domain inhibited the maximum InsP signal for SFLLRN and caused a slight right shift in the EC_{50} for thrombin (Fig. 2, *C* and *D*). In contrast, the BicD1ct domain had no effect on the ability of the PAR4 ligand,

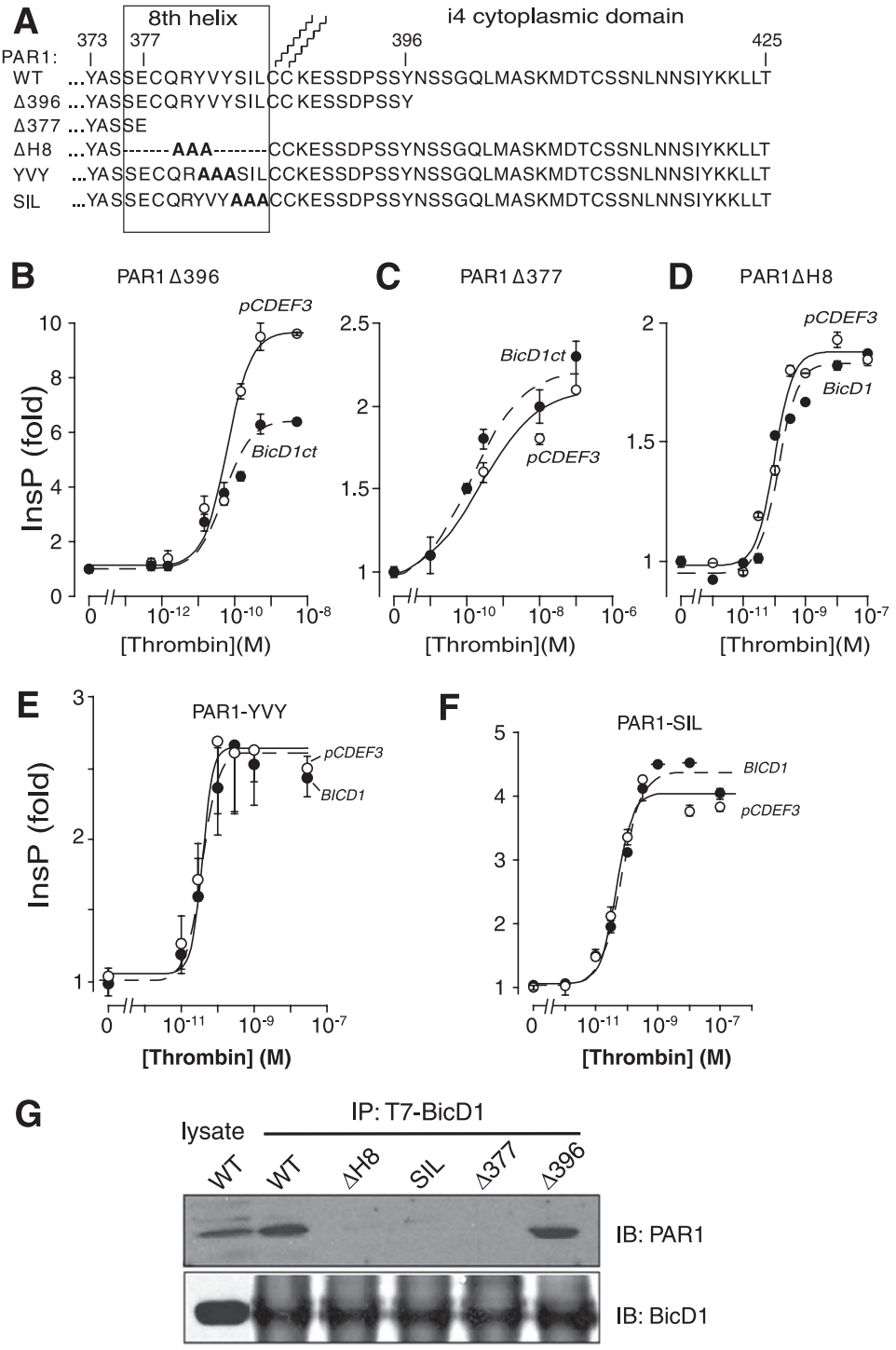

FIGURE 3. **BicD1 inhibits G protein signaling through its interaction with the 8th helix of PAR1.** *A*, C-terminal sequences of the PAR1 C-terminal domain and 8th helix mutants are shown. The *two jagged lines* over C387C388 represent putative palmitoylation sites. *B–F*, PAR1 mutants were co-transfected into COS7 cells along with GFP-BicD1ct (BicD1ct), full-length BicD1 (1–873 aa), or pCDEF3 vector control as indicated. Cells were then challenged for 30 min with 1 pM to 100 nM thrombin (each *point* done in triplicate), and PLC-β activity was determined by measuring total [^{3}H]InsP formation and converted to fold response relative to buffer alone ($n = 3$). Data are plotted as mean ± 1 S.D. (*error bars*). *G*, co-immunoprecipitation (*IP*) of BicD1 with PAR1 requires an intact 8th helix of PAR1. COS7 cells were transiently transfected with PAR1 mutants and full-length T7-BicD1. Lysates from transfected COS7 were incubated with T7-agarose beads and proteins in lysate, and immunoprecipitation eluates were separated by 10% SDS-PAGE, and Western blot analysis (*IB*) using the SFLLR and BicD1 antibodies were performed.

AYPGDF, to stimulate PAR4 signaling (Fig. 2*E*). Full-length BicD1 had no effect on InsP signaling from the closely homologous PAR2, nor on SST2, CCKA, or CCKB receptors in this heterologous expression system (Fig. 2*F*). These data indicate that BicD1 specifically modulates PAR1 signaling.

Identification of the 8th Helix of PAR1 as the Site of Interaction with BicD1—To narrow down the regions of PAR1 involved in the signal inhibition by BicD1, we made serial truncations of the cytoplasmic i4 domain of PAR1 (Fig. 3*A*). The PAR1Δ396 mutant lacks the last 29 residues of PAR1 and is missing the sites of serine and threonine phosphorylation required for desensitization of PAR1 by receptor-dependent kinases (17). Interestingly, the BicD1ct domain could still efficiently inhibit InsP signaling from the PAR1Δ396 mutant (Fig. 3*B*). In contrast, β-arrestin-1 had no effect on the signaling of PAR1Δ396 but could inhibit 50% of the signal from wild-type PAR1 (data not shown) as reported previously (28). As expected, truncation of the entire i4 domain (PAR1Δ377) removed the inhibitory effects of BicD1 (Fig. 3*C*). Previous studies have shown that the 8th helix of PAR1 located in the N-terminal portion of the i4 domain of PAR1 is essential for signaling to G_q (27). Although the signal generated by the PAR1ΔH8 mutant was reduced relative to wild-type because of the loss of G protein-interacting residues, co-expression with BicD1 gave no further inhibition of the G_q-InsP signal (Fig. 3*D*).

To probe the PAR1 8th helix-BicD1 interaction further, triple-alanine substitutions were made to disrupt potential coiled-coil interactions with BicD1. Both the PAR1 YVY/AAA and SIL/AAA mutations prevented BicD1 from inhibiting PAR1-G protein signaling (Fig. 3, *E* and *F*), indicating that these PAR1 8th helix residues are essential for the interaction with BicD1. To rule out the possibility that the PAR1 signaling was influenced due to the altered receptor surface expression levels caused by co-transfection of BicD1, we quantified surface expression of all of the PAR1 mutants using FACS. The data shown in supplemental Fig. 1 indicate that co-expression with BicD1 or vector controls gave no significant differences in sur-

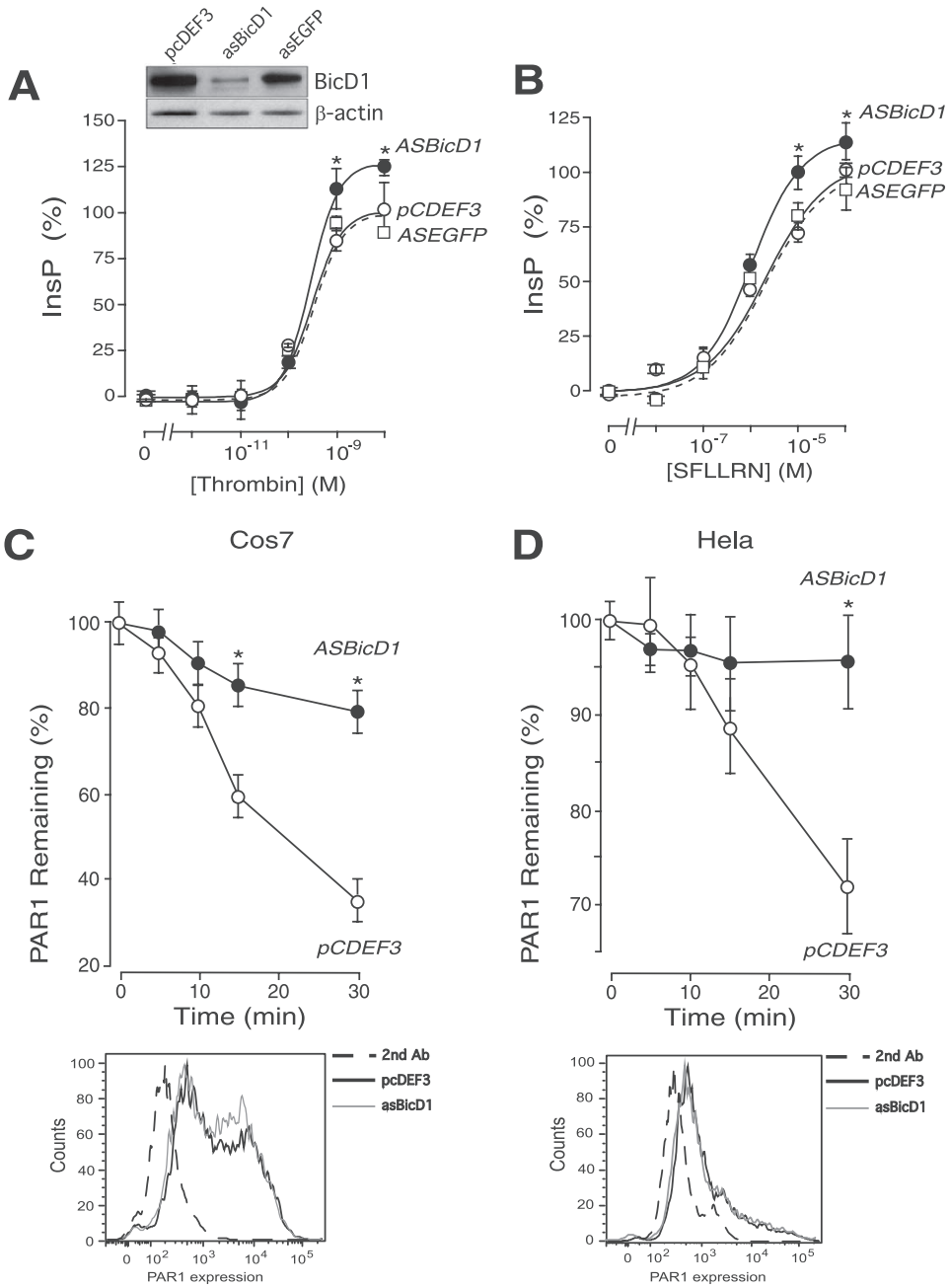

FIGURE 4. **Knockdown of BicD1 expression enhances PAR1-G protein signaling and inhibits endocytosis.** *A* and *B*, PAR1 was co-transfected into Rat1 cells along with antisense-BicD1 DNA, antisense-EGFP DNA, or pCDEF3 vector controls as indicated. Cells were then challenged for 30 min, or SFLLRN and PLC-β activity was determined by measuring total [^{3}H]InsP formation and converted to percent response relative to the maximal signal observed with pCDEF3 control ($n = 3$). Knockdown of BicD1 by asBicD1 was confirmed by Western blot analysis as shown in the *inset* in *A*. *C* and *D*, *upper*, endocytosis of PAR1 in COS7 cells (*C*) and HeLa cells (*D*) co-transfected with PAR1 and antisense BicD1 or pCDEF3 control vector is indicated. Loss of PAR1 SFLLR epitope from the cell surface was analyzed by flow cytometry as described previously (3). *Lower*, basal PAR1 surface expression levels of both COS7 and HeLa cells determined by FACS indicate that the surface expression levels of PAR1 in the antisense BicD1-transfected cells are not significantly different from control pcDEF3 cells. Data are plotted as mean $\pm$ 1 S.D. (*error bars*). *, $p < 0.05$.

face expression of wild-type (WT) PAR1 or PAR1 mutants. Therefore, it appears that BicD1 is regulating G protein coupling to PAR1 by suppressing the maximal signal strength and not by affecting PAR1 surface expression or coupling affinity to G protein.

To test directly the effect of loss or mutation of the PAR1 8th helix, co-immunoprecipitation of the PAR1 mutants was conducted with the T7-tagged BicD1. As shown in Fig. 3*G*, deletion of the entire i4 domain (Δ377) or specific deletion of the 8th helix (ΔH8) of PAR1 resulted in complete loss of interaction of BicD1 with PAR1. Likewise, the SIL/AAA mutation of the 8th helix ablated the interaction with BicD1. Conversely, the PAR1Δ396 mutant retained full binding of BicD1 (Fig. 3*G*). Together, these data indicate that the interaction of BicD1 with PAR1 is mediated by the 8th helix of PAR1 and that this interaction is required for BicD1 to inhibit signaling between PAR1 and G protein.

Suppression of Endogenous BicD1 Enhances PAR1 Signaling and Inhibits Endocytosis—Next, we tested whether knockdown of expression of endogenous BicD1 would affect PAR1-G protein signaling. Rat1 cells were chosen because they expressed significant amounts of endogenous BicD1 expression. An antisense BicD1 cDNA (asBicD1) was generated and was found to cause a knockdown of 70% when normalized to the β-actin loading control (Fig. 4*A*). This suppression of endogenous BicD1 caused a ~25% increase in the InsP signal by thrombin and SFLLRN ligands in the PAR1-expressing Rat1 fibroblasts. The asEGFP gave a minor knockdown of BicD1 when normalized to β-actin and had no effect on the InsP signal from WT PAR1 to either SFLLRN or thrombin agonists (Fig. 4*A*-B). The observed 25% increase in maximal PAR1 signaling following 70% suppression of BicD1 is consistent with the opposing effect of attenuating 30–40% of the PAR1 signal by overexpression of BicD1 in Fig. 2, *A* and *B*, in these recombinant systems.

Previous studies have shown that the i4 cytoplasmic domain of PAR1 regulates agonist-dependent endocytosis (18). To examine the effect of BicD1 on endocytosis, we suppressed endogenous BicD1 with the antisense construct and measured the loss of PAR1 surface expression following addition of agonist. The equal basal surface expression of PAR1 following co-transfection with asBicD1 or vector alone was confirmed by FACS (Fig. 4, *C* and *D*, *lower*). Knockdown of BicD1 caused a marked inhibition in the rate of PAR1 endocy-

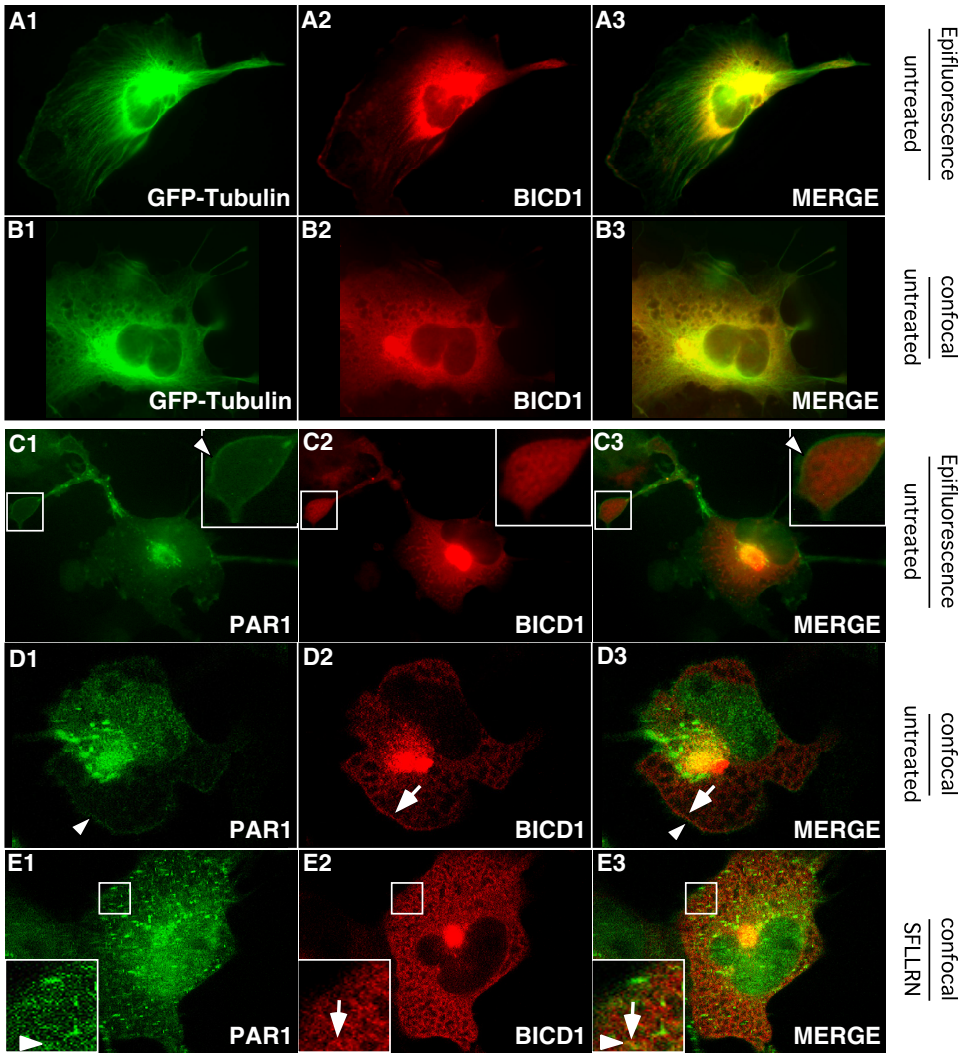

FIGURE 5. **Subcellular localization of BicD1 and PAR1.** COS7 cells were transfected with GFP-tubulin (*A* and *B*), PAR1 (*C–E*), and T7-BicD1 (*A–E*) and grown on coverslips. After 2 days, cells were fixed and stained with T7 antibody and SFLLRN antibody. *A* and *B*, epifluorescence (*A*) and confocal fluorescence microscopy (*B*) of untreated cells expressing BicD1 and GFP-tubulin. *C*, epifluorescence microscopy of untreated cells expressing PAR1 and BicD1. *D* and *E*, confocal microscopy of cells expressing BicD1 and PAR1 treated for 30 min with phosphate-buffered saline (*D*) or 30 μM SFLLRN (*E*).

tosis in both COS7 and HeLa cells (Fig. 4, *C* and *D*). Thus, BicD1 also regulates agonist-dependent endocytosis of PAR1.

Subcellular Localization of BicD1 and PAR1—Previous studies by Matanis *et al.* (25) showed that BicD1 interacts with the microtubule motor proteins dynein and dynactin, which are involved with movement of endosomes and other membrane vesicles. We confirmed that BicD1 extensively co-localizes with tubulin in COS7 cells by both fluorescence and confocal microscopy (Fig. 5, *A* and *B*). The localization of BicD in relation to PAR1 was also examined by fluorescence microscopy. Consistent with previous fluorescence studies (17), PAR1 localized to the plasma membrane in unstimulated fibroblasts. In addition, in the pseudopodial projections of fibroblasts, one can observe PAR1 localizing to the plasma membrane with BicD1 staining the adjoining area (Fig. 5, *C1–C3*). Similar results were obtained by confocal microscopy. PAR1 on the plasma membrane was found in close juxtaposition with the peripherally localized BicD1 which exhibited a honeycomb-like pattern in the cytoplasm (Fig. 5, *D1–D3*) in the unstimulated COS7 cells. The PAR1 agonist SFLLRN induced a redistribution of PAR1 from the plasma membrane to internal vesicles with substantial "orange" co-localization with BicD1 evident in Fig. 5*E3*, *merge*. BicD1 did not co-localize with PAR1 throughout the whole cell, which may reflect other non-PAR1 functions of BicD1 such as Rab6a-dependent Golgi-endoplasmic reticulum vesicle sorting (25).

BicD1 Is a Suppressor of PAR1-dependent Proliferation of Breast Carcinoma Cells—Previous studies have shown that PAR1 is a potent mitogenic factor and causes proliferation and tumorigenesis of breast carcinomas and other cell types (5, 29, 30). Given that BicD1 caused inhibition of PAR1-G protein signaling, we wondered whether suppression of endogenous BicD1 would enhance PAR1-dependent proliferation over a 3-day period. We transfected PAR1-null breast carcinoma cells, MCF-7, with WT PAR1 and antisense BicD1. As shown in Fig. 6, co-transfection of WT PAR1 with pcDEF3 vector control caused a 50% increase in the proliferation rate of the MCF-7 cells. Suppression of BicD1 with asBicD1 caused an additional 2-fold increase in the proliferation rate of the PAR1-transfected cells but had no discernable effect on the growth of the parental PAR1-null MCF-7 cells. The PAR1 ΔH8 mutant, which is defective in signaling to G_q and PLC-β, was also unable to enhance the proliferation of the MCF-7 cells over the 3-day time period. Additional transfection with asBicD1 had no effect on the PAR1 ΔH8 mutant. The PAR1 8th helix SIL/AAA triple mutant caused a nearly 2-fold increase in the proliferation rate, but as expected, the proliferation rate was not significantly enhanced by suppression of BicD1 because this mutant does not interact with PAR1. The PAR1Δ396 mutant was transfected into the MCF-7 cells. This mutant gives enhanced signaling to G proteins (Fig. 3) and caused a greater increase in proliferation relative to WT PAR1. Co-transfection of PAR1Δ396 with asBicD1 caused a further increase in proliferation as occurred with WT PAR1 (Fig. 6*A*).

Last, we tested whether agonist-stimulated PAR1 endocytosis was also affected by BicD1 silencing in the MCF-7 carcinoma cells. As shown in Fig. 6*B*, WT PAR1 surface expression was decreased by 40% 1 h after SFLLRN stimulation in the BicD1 group. A slight, but significant further decrease of PAR1

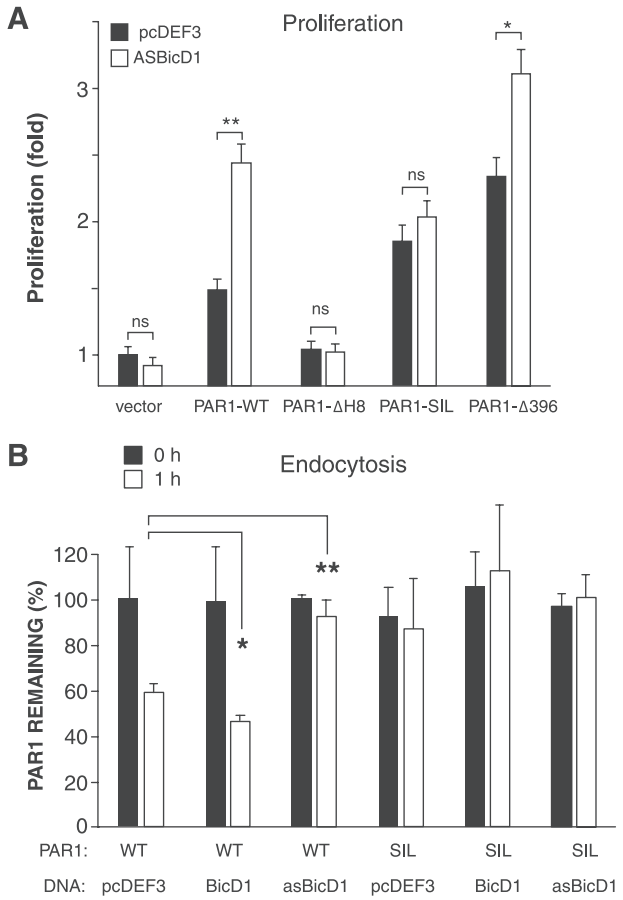

FIGURE 6. **Knockdown of BicD1 expression or mutation of the BicD1-interacting region of PAR1 enhances proliferation and modulates ligand-dependent endocytosis in MCF-7 breast carcinoma cells.** *A*, MCF-7 cells (2500/well) were transiently transfected with WT, ΔH8, SIL, or PAR1Δ396 along with pcDEF3 or asBicD1 in 96-well plates. After 48 h of transfection, cells were allowed to grow for another 72 h in RPMI 1640 serum-free medium, and proliferation was measured by 3-(4,5-dimethylthiazol-2-yl)-2,5-diphenyltetrazolium bromide assay ($n = 4$, mean ± S.D. (*error bars*)) as described previously (40). *B*, endocytosis of PAR1 in MCF-7 cells co-transfected with WT or SIL-PAR1 plus pcDEF3, BicD1, or asBicD1 is shown. Loss of PAR1 SFLLR-epitope from the cell surface was analyzed by flow cytometry as in Fig. 4. Data are plotted as mean ± 1 S.D. (*error bars*). *, $p < 0.05$; **, $p < 0.001$; *ns*, nonsignificant.

surface levels (53%) was observed when BicD1 was overexpressed. Quite strikingly, endocytosis of WT PAR1 was almost completely blocked by asBicD1 in the MCF-7 cells. In contrast, the PAR1 SIL mutant, which does not interact with BicD1, gave little or no endocytosis at 1 h after stimulation with SFLLRN, irrespective of co-transfection with asBicD1, overexpression of BicD1, or pcDEF3 vector control (Fig. 6*B*). Treatment with asBicD1 had no effect on WT or SIL mutant PAR1 basal surface expression in COS7 cells (supplemental Fig. 1) nor in MCF-7 cells (data not shown) by FACS. These data are consistent with the notion that BicD1 may in part affect PAR1-dependent proliferation of MCF-7 by reducing the turnover/endocytosis of PAR1 and that these effects require the interaction between BicD1 and the 8th helix of PAR1.

DISCUSSION

In the present work, we identified BicD1 as a novel regulator of PAR1-G protein signaling, internalization, and proliferation. *BICD* has long been known as an essential developmental gene in *Drosophila* oocytes. Mutations in *BICD* disrupt the polarity of the early embryo, which results in the formation of the Bicaudal or double abdomen phenotype (31). BicD1 was found to transport mRNA transcripts and regulate retrograde transport of vesicles from the Golgi to the endoplasmic reticulum (24, 25). BicD1 is a highly α-helical protein and consists of three coiled-coil domains with leucine zippers and heptad repeats (32). The coiled-coil domains of BicD1 and related isoform BicD2 interact with proteins involved in vesicle trafficking such as Rab6a, dynein, and dynactin, and signaling molecules such as misshapen, GSK-3β, and Nek8 (25, 33–35). In human platelets, dynein was found to be translocated and phosphorylated upon thrombin activation, providing independent evidence that the dynein microtubule motor protein might be involved in PAR1 signaling and internalization (36). We found that the cytoplasmic tail of PAR1 interacted with the CC3 coiled-coil domain of BicD1. This interaction was confirmed by immunoprecipitation and immunofluorescence microscopy. Furthermore, BicD1 co-localized with tubulin, which is consistent with the role of BicD1 in vesicular transport.

Several studies have examined the mechanism of PAR1 endocytosis and have found that the internalization of PAR1 involves a clathrin- and dynamin-dependent pathway that is independent of β-arrestins (17, 18, 37). Previous work also showed that β-arrestin-1 can interfere with coupling between PAR1 and G proteins (17, 28). Unlike β-arrestin-1, the BicD1 CC3 domain could still inhibit signaling of the truncated PAR1 mutant Δ396. PAR1Δ396 is defective in receptor phosphorylation (15) but still strongly interacts with BicD1. Thus, BicD1 appears to inhibit PAR1 signaling through a mechanism independent of β-arrestin.

The work here also suggests that BicD1 serves as an adapter protein that bridges activated PAR1 with the endocytosis machinery. Thus, knockdown of BicD1 expression nearly completely eliminated endocytosis of ligand-activated PAR1. Mutational analysis of PAR1 identified the region between residues 377 and 396 as essential for binding to BicD1. This membrane-proximal region of the PAR1 cytoplasmic tail contains an 8th helix (27) that might form coiled-coil interactions with the BicD1 CC3 coiled-coil domain. Deletion of the 8th helix as well as interruption of coiled-coil interactions by alanine substitution (PAR1YVY/AAA and PAR1SIL/AAA) ablated the ability of BicD1 to bind PAR1 and inhibit G protein signaling. These data are in agreement with previous studies that showed that similar point mutations in the 8th helix caused severe impairment of PAR1 endocytosis (37). Therefore, BicD1 is likely to form a coiled-coil interaction with the 8th helix of the PAR1 cytoplasmic tail, and this interaction is required for endocytosis.

Both the BicD1 CC3 domain and full-length BicD1 inhibited PLC-β signaling upon thrombin or SFLLRN activation in COS7 cells. PAR1 signals to PLC-β in COS7 cells via G_q (27). The 8th helix region of the PAR1 C-terminal i4 domain is essential for signal transference to G_q (27). Therefore, it is highly likely that BicD1 and G_q compete or overlap for the same binding site on PAR1. In this regard, there appears to be stronger inhibition of PAR1 signaling by BicD1 with SFLLRN activation compared

with thrombin activation. The peptide-activated PAR1 has been shown to couple preferentially to G_q compared with thrombin-activated PAR1 (38, 39). These apparent differences may be due to different conformational changes that occur in the PAR1 cytoplasmic domains upon thrombin *versus* SFLLRN activation.

PAR1 strongly stimulates DNA synthesis and proliferation by activating extracellular signal-regulated kinase/mitogen-activated protein kinase signaling cascades (29). We found that ectopic expression of PAR1 caused a 50% increase in the basal growth rate of PAR1-null MCF-7 breast carcinoma cells. Suppression of BicD1 expression caused a dramatic increase in PAR1-driven proliferation that was observed in WT and the phosphorylation-defective Δ396 mutant PAR1, which had an even further elevation in the rate of proliferation. Likewise, the 8th helix SIL mutant that lost BicD1 binding exhibited a high basal proliferation rate that was not affected by loss of BicD1 expression. The suppressive effect of BicD1 on PAR1-induced proliferation may be due at least in part to the ability of BicD1 to internalize PAR1 because BicD1 knockdown inhibited ligand-dependent endocytosis without affecting basal surface expression. Together, these data indicate that BicD1 can suppress PAR1 in the context of G protein signaling, receptor internalization, and cancer cell proliferation.

Acknowledgments—We thank Dr. Marc Vidal (Dana-Farber) for kindly providing the yeast strains and plasmids and for advice on the yeast two-hybrid methodologies, and we thank Robb Wilson of the Tufts GRASP center for assistance in collecting the confocal images.

REFERENCES

1. Ossovskaya, V. S., and Bunnett, N. W. (2004) *Physiol. Rev.* **84,** 579–621
2. Vu, T.-K. H., Hung, D. T., Wheaton, V. I., and Coughlin, S. R. (1991) *Cell* **64,** 1057–1068
3. Kuliopulos, A., Covic, L., Seeley, S. K., Sheridan, P. J., Helin, J., and Costello, C. E. (1999) *Biochemistry* **38,** 4572–4585
4. Riewald, M., Petrovan, R. J., Donner, A., Mueller, B. M., and Ruf, W. (2002) *Science* **296,** 1880–1882
5. Boire, A., Covic, L., Agarwal, A., Jacques, S., Sherifi, S., and Kuliopulos, A. (2005) *Cell* **120,** 303–313
6. Trivedi, V., Boire, A., Tchernychev, B., Kaneider, N. C., Leger, A. J., O'Callaghan, K., Covic, L., and Kuliopulos, A. (2009) *Cell* **137,** 332–343
7. Seeley, S., Covic, L., Jacques, S. L., Sudmeier, J., Baleja, J. D., and Kuliopulos, A. (2003) *Chem. Biol.* **10,** 1033–1041
8. Dhanasekaran, N., Tsim, S. T., Dermott, J. M., and Onesime, D. (1998) *Oncogene* **17,** 1383–1394
9. Leger, A. J., Covic, L., and Kuliopulos, A. (2006) *Circulation* **114,** 1070–1077
10. Pawlinski, R., Tencati, M., Hampton, C. R., Shishido, T., Bullard, T. A., Casey, L. M., Andrade-Gordon, P., Kotzsch, M., Spring, D., Luther, T., Abe, J., Pohlman, T. H., Verrier, E. D., Blaxall, B. C., and Mackman, N. (2007) *Circulation* **116,** 2298–2306
11. Brzostowski, J. A., and Kimmel, A. R. (2001) *Trends Biochem. Sci.* **26,** 291–297
12. Luttrell, L. M., and Lefkowitz, R. J. (2002) *J. Cell Sci.* **115,** 455–465
13. DeFea, K. A., Zalevsky, J., Thoma, M. S., Déry, O., Mullins, R. D., and Bunnett, N. W. (2000) *J. Cell Biol.* **148,** 1267–1281
14. Ishii, K., Chen, J., Ishii, M., Koch, W. J., Freedman, N. J., Lefkowitz, R. J., and Coughlin, S. R. (1994) *J. Biol. Chem.* **269,** 1125–1130
15. Hammes, S. R., and Coughlin, S. R. (1999) *Biochemistry* **38,** 2486–2493
16. Tiruppathi, C., Yan, W., Sandoval, R., Naqvi, T., Pronin, A. N., Benovic, J. L., and Malik, A. B. (2000) *Proc. Natl. Acad. Sci. U.S.A.* **97,** 7440–7445
17. Paing, M. M., Stutts, A. B., Kohout, T. A., Lefkowitz, R. J., and Trejo, J. (2002) *J. Biol. Chem.* **277,** 1292–1300
18. Marchese, A., Paing, M. M., Temple, B. R., and Trejo, J. (2008) *Annu. Rev. Pharmacol. Toxicol.* **48,** 601–629
19. Trejo, J., Hammes, S. R., and Coughlin, S. R. (1998) *Proc. Natl. Acad. Sci. U.S.A.* **95,** 13698–13702
20. Wang, Y., Zhou, Y., Szabo, K., Haft, C. R., and Trejo, J. (2002) *Mol. Biol. Cell* **13,** 1965–1976
21. Trejo, J., Altschuler, Y., Fu, H. W., Mostov, K. E., and Coughlin, S. R. (2000) *J. Biol. Chem.* **275,** 31255–31265
22. Wharton, R. P., and Struhl, G. (1989) *Cell* **59,** 881–892
23. Mach, J. M., and Lehmann, R. (1997) *Genes Dev.* **11,** 423–435
24. Bullock, S. L., and Ish-Horowicz, D. (2001) *Nature* **414,** 611–616
25. Matanis, T., Akhmanova, A., Wulf, P., Del Nery, E., Weide, T., Stepanova, T., Galjart, N., Grosveld, F., Goud, B., De Zeeuw, C. I., Barnekow, A., and Hoogenraad, C. C. (2002) *Nat. Cell Biol.* **4,** 986–992
26. Claussen, M., and Suter, B. (2005) *Ann. Anat.* **187,** 539–553
27. Swift, S., Leger, A. J., Talavera, J., Zhang, L., Bohm, A., and Kuliopulos, A. (2006) *J. Biol. Chem.* **281,** 4109–4116
28. Chen, C. H., Paing, M. M., and Trejo, J. (2004) *J. Biol. Chem.* **279,** 10020–10031
29. Van Obberghen-Schilling, E., Vouret-Craviari, V., Chen, Y. H., Grall, D., Chambard, J. C., and Pouysségur, J. (1995) *Ann. N.Y. Acad. Sci.* **766,** 431–441
30. Zain, J., Huang, Y. Q., Feng, X., Nierodzik, M. L., Li, J. J., and Karpatkin, S. (2000) *Blood* **95,** 3133–3138
31. Baens, M., and Marynen, P. (1997) *Genomics* **45,** 601–606
32. Stuurman, N., Häner, M., Sasse, B., Hübner, W., Suter, B., and Aebi, U. (1999) *Eur. J. Cell Biol.* **78,** 278–287
33. Holland, P. M., Milne, A., Garka, K., Johnson, R. S., Willis, C., Sims, J. E., Rauch, C. T., Bird, T. A., and Virca, G. D. (2002) *J. Biol. Chem.* **277,** 16229–16240
34. Houalla, T., Hien Vuong, D., Ruan, W., Suter, B., and Rao, Y. (2005) *Mech. Dev.* **122,** 97–108
35. Fumoto, K., Hoogenraad, C. C., and Kikuchi, A. (2006) *EMBO J.* **25,** 5670–5682
36. Rothwell, S. W., and Calvert, V. S. (1997) *Thromb. Haemost.* **78,** 910–918
37. Paing, M. M., Temple, B. R., and Trejo, J. (2004) *J. Biol. Chem.* **279,** 21938–21947
38. Vouret-Craviari, V., Van Obberghen-Schilling, E., Rasmussen, U. B., Pavirani, A., Lecocq, J. P., and Pouysségur, J. (1992) *Mol. Biol. Cell* **3,** 95–102
39. McLaughlin, J. N., Shen, L., Holinstat, M., Brooks, J. D., Dibenedetto, E., and Hamm, H. E. (2005) *J. Biol. Chem.* **280,** 25048–25059
40. Kamath, L., Meydani, A., Foss, F., and Kuliopulos, A. (2001) *Cancer Res.* **61,** 5933–5940